Chemical Physics 178 (1993) 505–514
North-Holland

Study of isotope effects in the ground state of the symmetrical isotopomers of $CuCl_2$

P. Crozet, J.C. Coste, R. Bacis, A.J. Bouvier, S. Churassy and A.J. Ross
Laboratoire de Spectrometrie Ionique et Moleculaire (URA du CNRS No. 171), Université Lyon I, Bâtiment 205, 43 Bd du 11 Novembre 1918, 69622 Villeurbanne, France

Received 7 June 1993

Investigations of the ground state of $CuCl_2$ have been pursued, recording laser induced fluorescence spectra on a Bomem DA3 Fourier transform spectrometer in the range 10000–16500 cm^{-1}. A single mode ring dye laser, set in the red (615–665 nm), excited the $^2\Pi_u$–$\tilde{X}\,^2\Pi_g$ electronic transition in copper dichloride vapour. Analysis of spectra recorded from isotopically enriched samples of $CuCl_2$ allowed us to check our assignment of vibrational stretching quantum numbers $v_1(\leqslant 7)$ and $v_3(\leqslant 8)$ in the ground state. A normal mode model including isotope effects has been used to fit data from all four symmetrical isotopomers of copper dichloride. The rms deviation of the fit containing about 4000 lines is 0.040 cm^{-1}. From this model, we find an equilibrium Cu–Cl bond length of 0.203335(5) nm and force constant $k_1 = 277.28(1)$ N m^{-1}.

1. Introduction

Thirty years ago, $CuCl_2$ had already attracted interest because its electronic structure is one of the simplest to be found among the transition metal dihalides [1]. Moreover, $CuCl_2$ is easily produced in the vapour phase, and is a good candidate for testing ligand field theory on d-electron systems. Recent ab initio calculations [2], taking into account low-lying ligand field and charge transfer states, have provided a useful framework for the spectroscopic exploration of this molecule.

A specific interest in the spectroscopy of $CuCl_2$ arose when Yoshida et al. [3,4] suggested that this molecule was in some way involved in an energy transfer process occurring during the reaction of chemically generated $O_2(^1\Delta_g)$ and Cl_2 on heated copper (200°C). The formation of $CuCl_2$ in the presence of $O_2(^1\Delta_g)$ is accompanied by strong red emission [5] and weak infrared emission, and gives spectra [6] in the red (12000–16000 cm^{-1}) and in the near infrared (6500–9000 cm^{-1}). Strong similarities are observed between these spectra and emission or absorption spectra of copper dichloride in the vapour phase [7]. It is now widely accepted that this molecule is responsible for the infrared emission [8], and at least partly responsible for the red emission [9], although the phenomenon has not yet been properly explained. A full understanding of the excitation mechanism underlying the chemiluminescence requires a better knowledge of the electronic states of $CuCl_2$ involved in the reaction described above.

In a recent contribution [10], we presented a high resolution spectroscopic study of the ground state of $CuCl_2$ using the combined Fourier transform spectrometry (FTS) and laser induced fluorescence (LIF) techniques. Two sets of constants for $^{63}Cu^{35}Cl_2$ were presented from the analysis of P–R doublets which were observed in vibrational progressions to ground state levels of the symmetric stretch in combination with the antisymmetric stretch mode. First, band-by-band fits were used to obtain effective spectroscopic constants of the vibrational levels involved in the electronic transition, allowing individual lines to be recalculated to better than 0.010 cm^{-1} in the unperturbed regions. Then a simple polynomial expression for the ground state energy levels was used to fit the fluorescence data, using rotational constants of the two upper state levels found in the first step. The resulting rms deviation (0.14 cm^{-1}) reflects the occurrence of local perturbations, as shown in fig. 4 of ref. [10].

In this paper, we calculate an improved set of molecular constants relating to the lowest vibrational levels of the ground state of copper dichloride, attributed [10] to $^2\Pi_{g(3/2)}$. The data set has been increased considerably. In particular, care has been taken to record fluorescence close to the laser line, and even anti-Stokes fluorescence, so that the lowest vibrational level was well represented in the data set. This was one of the short-comings of our earlier work, where the effective constants of the ground state levels with $v_1=0$ and 1 were often derived from very few lines. This necessarily affected the accuracy of the equilibrium constants which were presented. We have now acquired an extensive block of data for the molecule $^{63}Cu^{37}Cl_2$, balancing the original data set for $^{63}Cu^{35}Cl_2$. We have deliberately confined our numerical treatment to the low-lying, essentially unperturbed vibrational levels, with $v_1 \leqslant 7$ and $v_3 \leqslant 8$, under which conditions simple isotopic relationships should be applicable. The vibrational numbering is established for the four symmetrical isotopic species of $CuCl_2$ using our polynomial model for the $^2\Pi_g$ state, which takes into account vibrational anharmonicities, vibration–rotation constants and isotopic factors. A small correction (0.01%) on one of the isotope factors has been found to improve significantly the quality of this polynomial fit. This correction parameter is also discussed and force constants are calculated in the valence force field model (VFF).

2. Experimental

The experimental arrangement has been described in detail in previous work (ref. [10], and fig. 1 of this reference). The sources are sealed quartz cells (length 180 mm, inner diameter 19 mm) ended by two Brewster windows and equipped with a sidearm. They were filled after outgassing the cell for a few hours on a 10^{-6} Torr vacuum line. $CuCl_2$ is prepared by heating copper wire (10 mg electrolytic Cu) in the presence of chlorine gas in the evacuated cell. A small excess of Cl_2 is maintained before sealing the cell in order to drive the equilibrium $CuCl_2 \rightleftharpoons CuCl + \frac{1}{2}Cl_2$ to the left. For isotopic studies, enriched samples of ^{63}Cu (C.E.A. Saclay, 99.9%) and of $^{37}Cl_2$ (Euriso-Top, groupe C.E.A., 95%) were used. One cell was prepared with natural Cu reacting with $^{37}Cl_2$, and then introducing 10 Torr of argon before sealing. This was intended to increase rotational relaxation processes, and did so quite successfully. During our experiments, the cell was heated in a dual temperature electric oven, typically at 750°C for the body of the cell, and 500°C for the sidearm. The lower temperature sets the $CuCl_2$ vapour pressure and the higher one favours the dissociation of copper dichloride dimer [11].

The $CuCl_2$ excitation is obtained from a cw ring dye laser (Spectra Physics 380-D), pumped by an argon ion laser (Spectra Physics 2045). Single mode operation is achieved by means of a temperature controlled reference cavity of 500 MHz free spectral range (Spectra Physics 388), which provides $\leqslant 1$ MHz linewidth and prevents mode hopping for a period of about 1 hour, with a frequency drift lower than 50 MHz/hour. Two dyes allowed us to use excitation wavenumbers in the range 15100–16250 cm^{-1}: rhodamine 6G and DCM. The excitation wavenumbers were chosen somewhat arbitrarily, and our investigation of the excitation spectrum in this region is far from being complete. The laser mode was monitored by a 2 GHz confocal interferometer (finesse 150) and the laser wavelength was measured continuously on a Fizeau-wedge wavemeter (Laser Technics 100).

Backwards LIF, collected by a pierced aluminium mirror, was focused by a 20 cm focal length lens, into a fused silica optical fibre (1 mm core, 10 m length), whose output matched the entrance iris of the Michelson interferometer (Bomem DA3). Fluorescence spectra were recorded in the range 10000–16500 cm^{-1} on a silicon-avalanche type detector, with an apodized resolution of 0.070 cm^{-1}, which represented a good detection compromise between acceptable recording times and the expected Doppler line width for $CuCl_2$ (about 0.030 cm^{-1} at 1000 K). In most experiments, an appropriate optical filter was used to attenuate the laser line, but in several instances the level of scattered light from the ring laser was low enough to allow recording without any filter to protect the detector, giving access to the anti-Stokes side of the LIF spectrum. With isotopically pure samples (e.g. $^{63}Cu^{37}Cl_2$), the signal/noise ratio of the Fourier transform records was appreciably better, allowing us to reduce the recording time to about one hour for a given laser excitation.

3. Laser induced fluorescence spectra

3.1. Upper levels

The intensity pattern of $CuCl_2$ LIF spectra is mainly dictated by the Franck–Condon factors on the symmetric stretch quantum numbers, as shown in fig. 1. So far, we have observed three different patterns, according to the frequency range of the ring dye laser, and the upper level attributed to the pump transition. These intensity profiles are plotted in fig. 1 for three excitation lines at similar J' values in $^{63}Cu^{37}Cl_2$:

$J'=68\frac{1}{2}$, $\nu_{\mathrm{laser}}=15170.47\ \mathrm{cm}^{-1}$,

which pumps $v'=0$ via $R(67\frac{1}{2})$ from $(1\,0\,0)$,

$J'=65\frac{1}{2}$, $\nu_{\mathrm{laser}}=15500.00\ \mathrm{cm}^{-1}$,

which pumps $v'=1$ via $R(64\frac{1}{2})$ from $(1\,0\,0)$,

$J'=65\frac{1}{2}$, $\nu_{\mathrm{laser}}=16223.77\ \mathrm{cm}^{-1}$,

which pumps $v'=2$ via $R(64\frac{1}{2})$ from $(0\,0\,0)$.

Analysis of rotational relaxation lines appearing around P–R doublets (fig. 2) gives without ambiguity $\Delta J'=\pm 2, \pm 4, \ldots$ for the transfers within the upper state vibrational levels. This makes it easy to establish the rotational constant for the upper level involved. Three distinct rotational constants were obtained for each isotopomer, and we labelled the corresponding levels $v'=0, 1, 2$ according to their energy. However, there is no obvious vibrational energy pattern linking these levels, although the inertial rotational constants appear to be connected to one another at given v' by the ratio of the reduced masses of the isotopomers. So we have not been able to identify the vibrational quantum numbers in the upper state, $^2\Pi_u$.

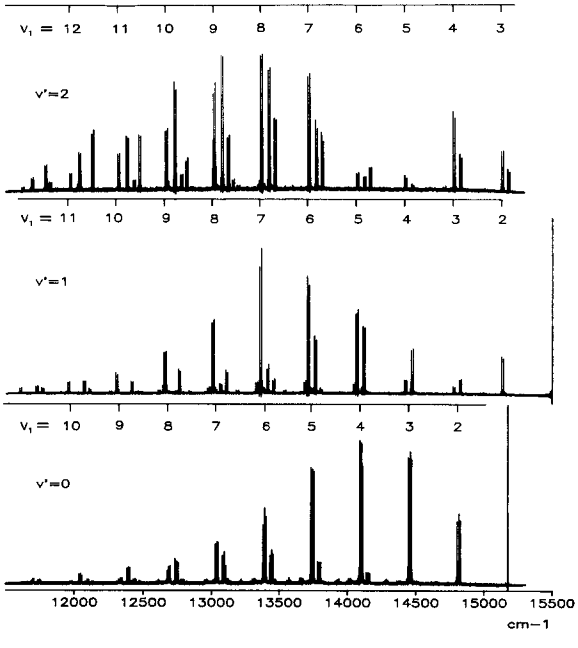

Fig. 1. Spectral intensity profiles for excited upper levels "$v'=0$, 1, 2" in the $^2\Pi_u$ state of $^{63}Cu^{37}Cl_2$, for laser pump lines 1^0_1, 1^1_1, 1^2_0, with $J'=68\frac{1}{2}$, $J'=65\frac{1}{2}$, and $J'=65\frac{1}{2}$, respectively. Symmetric stretch v_1 numbering is given above each spectrum. Nomenclature: "1^0_1" corresponds to a vibronic transition between two electronic states of a polyatomic molecule, in which vibration 1 is excited to the $v=1$ level in the lower and the $v'=0$ level in the upper electronic state (from ref. [18]).

3.2. Isotopic shifts

Because our first experiments were carried out with ordinary copper dichloride, which contains natural abundances of copper and chlorine isotopes (^{63}Cu and ^{65}Cu in the ratio 7:3, and ^{35}Cl and ^{37}Cl in the ratio 3:1), an early priority was to identify correctly the isotopic species appearing in the FTS-LIF spectra. From our earlier data on $^{63}Cu^{35}Cl_2$, we could predict the vibrational and rotational isotopic shifts by calculating lower state molecular constants for each isotopomer. Isotopic substitution of chlorine has a marked effect on the symmetric stretch frequency and on the rotational constant, but exchanging one copper isotope for the other does not. Only the magnitude of the antisymmetric stretch vibration was sensitive to the copper isotope, and the appearance of fluorescence to lower state levels with $v_3 \neq 0$ was a necessary prerequisite for molecular identification. Which molecule was involved actually became obvious from certain combination differences which were clear on the spectra (fig. 3). For example, the characteristic variation in the combination differences on substituting ^{37}Cl for ^{35}Cl with either isotope of copper was a decrease of about 9.8 cm^{-1} between, for instance, $R(J)$ transitions to $(v_1\,0\,0)$ and

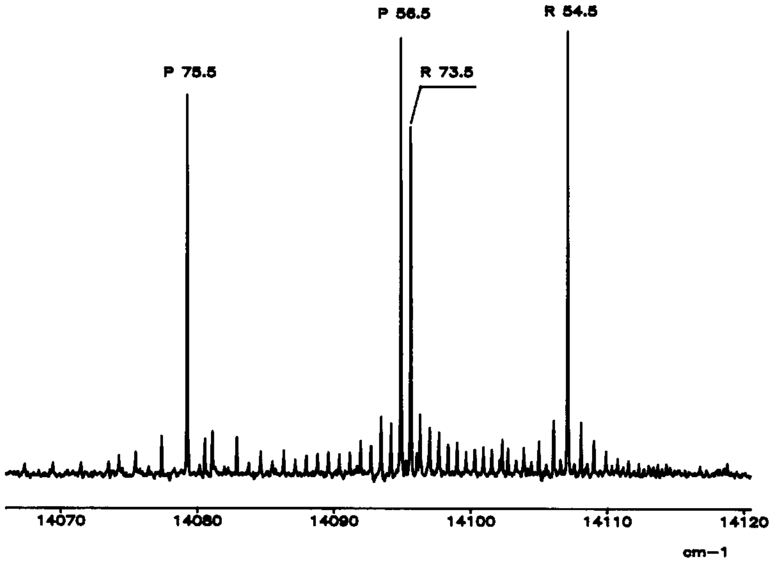

Fig. 2. Rotational relaxation lines around two fluorescence P–R doublets ($v_1=4$, $v_3=0$, $J'=55\frac{1}{2}$ and $74\frac{1}{2}$) in $^{63}Cu^{37}Cl_2$, pumped by $R(73\frac{1}{2})1_1^0$ and $P(56\frac{1}{2})1_1^0$ ($\nu_{laser}=15166.07$ cm^{-1}).

($v_1+1\,0\,0$), corresponding to the difference in one quantum of the symmetric stretch (fig. 3a). Substituting ^{65}Cu for ^{63}Cu in $Cu^{35}Cl_2$ produced an increase of about 8.2 cm^{-1} in the combination differences between, for example, transitions to ($v_1\,0\,0$) and ($v_1-3\,0\,2$) (fig. 3b).

4. Analysis and discussion

4.1. Model and results

From our previous hypothesis [10], the lower electronic level of our observed transitions is $^2\Pi_{g(3/2)}$. This has recently been independently confirmed [12]. The upper level is $^2\Pi_{u(3/2)}$ and the molecule is linear in both states. So the wavenumber of any fluorescence line can be represented by a difference in term energies for the upper and lower electronic states [13,14]. In the following, we use a vibrational label v' when we wish to refer the total vibration energy $T'_{v'}$ of the levels populated by the laser in the electronic excited state. J' is the true rotational quantum number in the $^2\Pi_u$ state. The lower state energy levels $T_{v_1,v_3}(J)$ are characterized in terms of three quantum numbers J, v_1 and v_3:

$$\nu_{\text{measured}}=T'_{v'}(J')-T_{v_1,v_3}(J)\,, \tag{1}$$

where

$$T'_{v'}(J')=T'_{v'}+B'_{v'}J'(J'+1)-D'_{v'}J'^2(J'+1)^2\,, \tag{2a}$$

$$\begin{aligned}T_{v_1,v_3}(J)=&\sum_{j=1,2,3}\omega_j(v_j+d_j/2)+x_{11}(v_1+\tfrac{1}{2})^2\\&+x_{33}(v_3+\tfrac{1}{2})^2+x_{13}(v_1+\tfrac{1}{2})(v_3+\tfrac{1}{2})\\&+x_{111}(v_1+\tfrac{1}{2})^3+x_{113}(v_1+\tfrac{1}{2})^2(v_3+\tfrac{1}{2})\\&+x_{133}(v_1+\tfrac{1}{2})(v_3+\tfrac{1}{2})^2+x_{333}(v_3+\tfrac{1}{2})^3\\&+\Big(B_e-\sum_{j=1,2,3}\alpha_j(v_j+d_j/2)\Big)J(J+1)\\&-\Big(D_e+\sum_{j=1,2,3}\beta_j(v_j+d_j/2)\Big)J^2(J+1)^2\,.\end{aligned} \tag{2b}$$

The degeneracy of the different vibrational modes appears in the d_j terms: $d_1=d_3=1$ and $d_2=2$. The parameter ω_2 is held fixed at a plausible numerical value which has been derived from a few very weak lines appearing in the fluorescence spectrum and which are believed to be transitions to ground state levels ($v_1\,2\,0$); the absence of strong progressions in the vibrational bending mode in our LIF spectra confirms the linear structure of $CuCl_2$ obtained by Bau-

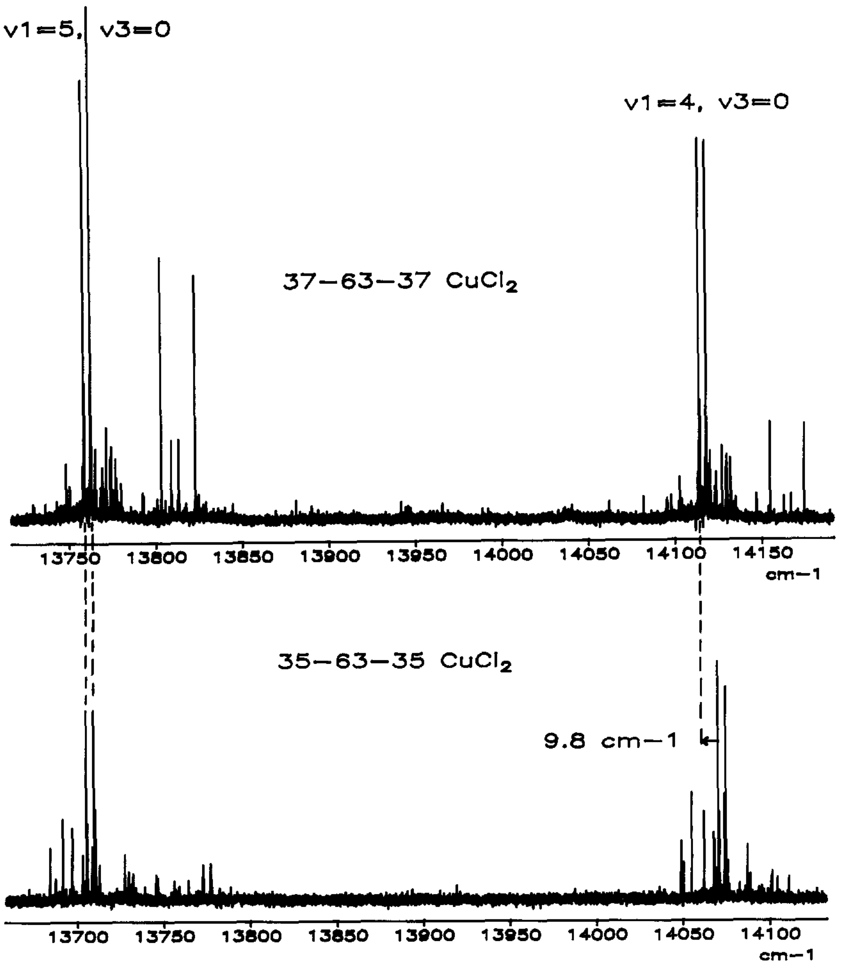

Fig. 3. (a) Effect of chlorine substitution on combination difference $(v_1, v_3=0)-(v_1+1, v_3=0)$, for two successive $J'=18\frac{1}{2}$ fluorescence P–R doublets. The $(v_1=5, v_3=0)$ doublets of the two isotopic species have been superposed by translating the $^{63}Cu^{37}Cl_2$ spectrum 53 cm^{-1} to low wavenumbers.

schlicher and Roos [2]. Our spectral data have been fitted with the polynomial model using a classical least squares fit routine, written in Turbo Pascal on a PC microcomputer, and transferred into a workstation when parameter matrix and data base dimensions increased. This program uses the same set of parameters to fit data from the four symmetrical isotopomers of copper dichloride, obtainable from isotopes ^{63}Cu, ^{65}Cu, $^{35}Cl_2$, and $^{37}Cl_2$. Before running the program, isotopic vibrational correction factors are set to numerical values calculated from the valence force field (VFF) model for a linear XY_2 molecule [13]:

$$\omega_j^{(i)}=\rho_j\omega_j,\quad x_{jk}^{(i)}=\rho_j\rho_k x_{jk},\quad x_{jkl}^{(i)}=\rho_j\rho_k\rho_l x_{jkl},\qquad (3)$$

where $\rho_1=\rho_2=\rho_3=1$ for $^{63}Cu^{35}Cl_2$; the superscript (i) is an index identifying the isotopomer; ω_j are the zeroth-order frequencies; $j, k, l=1$ (symmetric stretch), 2 (bending), or 3 (antisymmetric stretch);

$$\rho_1=(m_Y/m_Y^{(i)})^{1/2};$$

$$\rho_2=\rho_3=\left(\frac{(m_Y/m_Y^{(i)})(1+2m_Y^{(i)}/m_X^{(i)})}{1+2m_Y/m_X}\right)^{1/2}.\qquad (4)$$

The rotational correction formulae are [14]

$$B_e^{(i)}=\rho^2B_e,\quad \alpha_1^{(i)}=\rho^2\rho_1\alpha_1,\quad \alpha_3^{(i)}=\rho^2\rho_3\alpha_3,\qquad (5a)$$

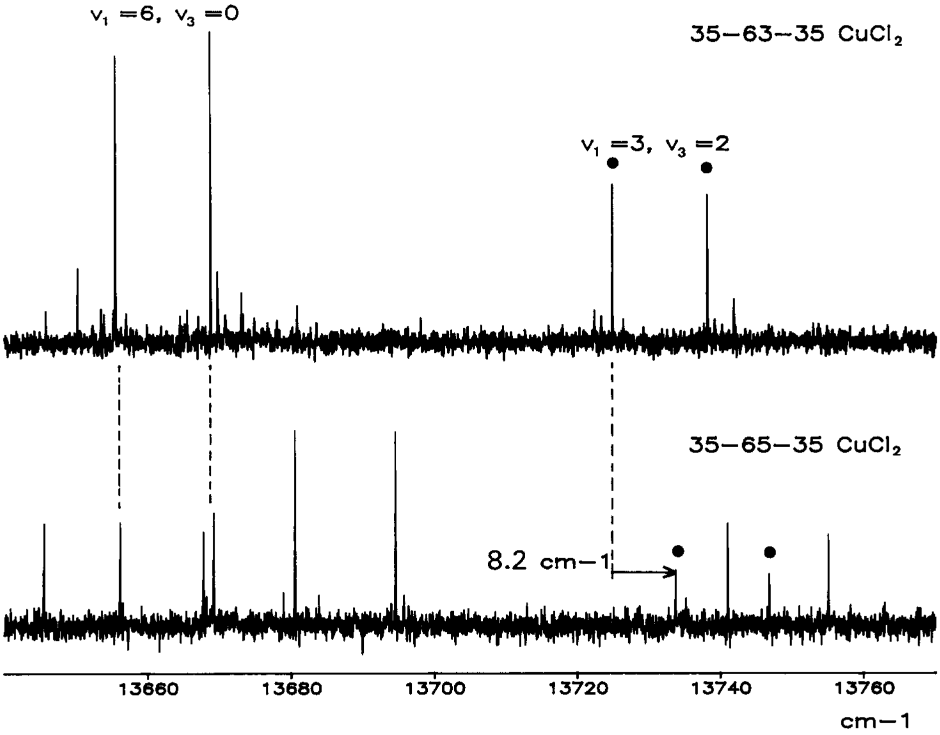

Fig. 3. (b) Effect of copper substitution on combination difference $(v_1-3, v_3=2)-(v_1, v_3=0)$, for two successive $J'=56\frac{1}{2}$ fluorescence P–R doublets. The wavenumber scale is the same for both spectra.

$$D_e^{(i)}=\rho^4 D_e,\quad \beta_1^{(i)}=\rho^4\rho_1\beta_1,\quad \beta_3^{(i)}=\rho^4\rho_3\beta_3, \tag{5b}$$

$$\rho=(m_Y/m_Y^{(i)})^{1/2}\,. \tag{5c}$$

Because we wanted to use the isotope effect to establish the vibrational numbering in v_1 and v_3, we incremented these quantum numbers and studied the effect on the rms deviation of the fit in table 1 (we studied also the effect of shifting J from our original numbering, in table 2). At this stage, there was a feeble minimum (0.005 cm^{-1}) in the root mean square deviation obtained by increasing v_3 by 1. This would imply that all our data originated from levels (0 0 1) or (1 0 1) instead of (0 0 0) or (1 0 0). The vibrational energies are of the order of 526 cm^{-1}, and we suspected that the thermal distributions were unlikely to populate these levels so well. We therefore considered the problem from a different angle, and supposed that the isotopic correction might be slightly imperfect for the vibrational motion. In an attempt to test the accuracy of the VFF model, we introduced

Table 1
rms deviation (in 10^{-3} cm^{-1}) of the polynomial fit for various shifts on vibrational numbering [a]

Δv_3	Δv_1			
	0	+1	+2	+3
0	62	79	112	152
	40	**64**	**102**	**145**
1	58	87	126	168
	53	**85**	**124**	**167**
2	67	103	144	187
	76	**110**	**149**	**191**
3	87	125	166	209
	102	**136**	**175**	**216**

[a] Normal typeface: rms from standard [13,14] isotopic factors. Bold typeface: rms from corrected isotopic factors. Δv_1 and Δv_3 are increments applied on the original symmetric and antisymmetric stretch quantum numbering.

Table 2
rms deviation (in 10^{-3} cm^{-1}) of the polynomial fit for various shifts on rotational numbering [a]

ΔJ				
0	+1	−1	+2	−2
62	117	119	208	212
40	**108**	**108**	**204**	**205**

[a] Normal typeface: rms from standard [13,14] isotopic factors. Bold typeface: rms from corrected isotopic factors.

in the previous isotopic formulae, a correction factor on ρ_1, such that the new isotopic factor ρ'_1 is

$$\rho'_1 = \rho_1(1+\epsilon) . \tag{6}$$

The factor ϵ represents a correction from a classical diatomic model, as quoted for instance by Watson [15]. It has been chosen in order to minimize the rms deviation of the fit. Therefore all the molecular parameters involving ρ_1 had to be corrected. With the best ρ'_1 obtained, the effect on the rms error of the fit (table 1) gives a significantly better minimum when

Table 3
Molecular constants of $CuCl_2$ from polynomial fitting of the ground state [a]

	standard isotopic factors:	corrected isotopic factors:
	35–65–35: $\rho_1=1, \rho_2=\rho_3=0.991868$	35–65–35: $\rho_1=1, \rho_2=\rho_3=0.991868$
	37–63–37: $\rho_1=0.972614, \rho_2=\rho_3=0.987124$	37–63–37: $\rho_1=0.972770, \rho_2=\rho_3=0.987124$
	37–65–37: $\rho_1=0.972614, \rho_2=\rho_3=0.978885$	37–65–37: $\rho_1=0.972770, \rho_2=\rho_3=0.978885$
lower state constants (in cm^{-1})		
ω_1	$3.71673(9)\times10^{2}$	$3.71698(6)\times10^{2}$
x_{11}	$-4.946(22)\times10^{-1}$	$-5.056(14)\times10^{-1}$
x_{111}	$-1.40(16)\times10^{-3}$	$-4.9(10)\times10^{-4}$
ω_3	$5.25923(8)\times10^{2}$	$5.25921(5)\times10^{2}$
x_{33}	$-1.2212(18)$	$-1.2211(11)$
x_{333}	$1.93(13)\times10^{-3}$	$1.77(8)\times10^{-3}$
x_{13}	$-2.5743(20)$	$-2.5763(13)$
x_{113}	$-2.99(19)\times10^{-3}$	$-2.93(12)\times10^{-3}$
x_{133}	$6.13(18)\times10^{-3}$	$6.70(12)\times10^{-3}$
B_e	$5.82801(49)\times10^{-2}$	$5.82990(31)\times10^{-2}$
α_1	$1.216(10)\times10^{-4}$	$1.253(6)\times10^{-4}$
α_3	$1.954(11)\times10^{-4}$	$1.947(7)\times10^{-4}$
D_e	$4.4(7)\times10^{-9}$	$6.9(4)\times10^{-9}$
β_1	$1.8(15)\times10^{-10}$	$-3.4(10)\times10^{-10}$
β_3	$2.0(16)\times10^{-10}$	$3.7(10)\times10^{-10}$
upper state constants (in cm^{-1})		
$T'_{35-63-35}(0)$	16080.475(15)	16080.451(10)
$T'_{35-65-35}(0)$	16079.039(18)	16079.028(12)
$T'_{37-63-37}(0)$	16074.194(15)	16074.412(10)
$T'_{37-65-37}(0)$	16072.821(16)	16073.048(10)
$T'_{35-63-35}(1)$	16416.308(15)	16416.289(10)
$T'_{35-65-35}(1)$	16413.351(19)	16413.328(12)
$T'_{37-63-37}(1)$	16402.554(16)	16402.748(10)
$T'_{35-63-35}(2)$	16791.188(15)	16791.174(10)
$T'_{35-65-35}(2)$	16785.034(17)	16785.026(11)
$T'_{37-63-37}(2)$	16769.543(15)	16769.748(10)
rms deviation	0.062	0.040

[a] Data set: $v_1 \leqslant 7$, $v_2=0$, $v_3 \leqslant 8$, $5\frac{1}{2} \leqslant J \leqslant 99\frac{1}{2}$, number of lines = 3915. The rotational constants $B'(v')$ and $D'(v')$ for the upper state levels $v'=0$, 1, and 2 have been blocked to values calculated in the band-by-band fit (see table 5). Constant related to the bending vibrational mode has been kept fixed at value $\omega_2 = 86.4$ cm^{-1}, deduced from weak combination bands involving $v_2=2$, recorded in $^{63}Cu^{37}Cl_2$ STF-LIF spectra. α_2 constant was fixed to 0. No data were available for $T'_{37-65-37}(1)$ and $T'_{37-65-37}(2)$.

ν_3 is maintained at its original value. This result implies that our initial model was approximate, and a better fit can be obtained by simply applying a small correction in the isotopic formulae. The spectroscopic constants of the ground state of $CuCl_2$ calculated from the polynomial fit are given in table 3. The first column deals with the classical isotopic factors ρ, ρ_1, ρ_3, whereas the second takes into account ρ, ρ'_1, ρ_3. The numerical values of these factors are listed in this table. In table 4, the variations of the rms deviation are given versus ϵ. A minimum of 0.040 cm^{-1} is reached for $\epsilon = 1.6 \times 10^{-4}$, instead of 0.062 cm^{-1} from the classical model with $\epsilon = 0$. No change in the rms error of the fit was noted when the parameters ρ_2 and ρ_3 were altered by comparable values, so these isotopic factors are left unchanged (table 3). The behaviour of the three observed excited levels, labelled "$v' = 0$, 1, 2", is still unclear, which is reflected in tables 3 and 5. The three upper levels of the electronic transition have been treated with different spectroscopic constants T', B', D' for each isotopomer. B' and D' are fixed to the best values calculated by a level-by-level fit (table 5), while T' is a floating parameter.

Table 4
rms deviation of the polynomial fit versus isotopic correction factor ϵ

ϵ ($\times 10^{-4}$)	rms deviation ($\times 10^{-3}$ cm^{-1})
−0.1	64.5
0.0	62.2
0.1	60.0
0.2	57.8
0.5	51.7
1.0	43.8
1.5	40.0
1.6	39.8
1.7	39.9
1.8	40.2
1.9	40.7
2.0	41.4
2.5	47.6

4.2. Discussion

These results show an improvement by a factor of three in the rms deviation of the polynomial fit as compared with our previous data on $^{63}Cu^{35}Cl_2$ [10]. This comes from the use of new data on lower vibrational levels, combined with isotopic substitution data and a more rigorous rejection of perturbed lines.

The rms deviation of the fit is four times the rms deviation derived from the level-by-level fit. This observation can be explained by three factors. First, the inadequacy of the simple vibrational model: systematic differences, which are independent of the rotational quantum number, appear between experimental and calculated frequencies appears for some lower state levels, while this bias does not exist in the level-by-level fit, where there is no correlation between vibration-energy terms. Second, weak perturbations occuring at specific J values are encounted when studying the fit output in many vibrational bands. Third, isotopic relationships are only approximate.

Table 5
Rotational constants of the upper state of $CuCl_2$ from level-by-level fitting of fluorescence lines [a]

Upper level	Isotopomer	B' (cm^{-1})	D' (cm^{-1})
0	35–63–35	$5.1918(8) \times 10^{-2}$	$8.5(7) \times 10^{-9}$
0	35–65–35	$5.1919(20) \times 10^{-2}$	8.5×10^{-9}
0	37–63–37	$4.9117(13) \times 10^{-2}$	$6.3(15) \times 10^{-9}$
0	37–65–37	$4.9105(16) \times 10^{-2}$	$4.5(10) \times 10^{-9}$
1	35–63–35	$5.1768(14) \times 10^{-2}$	$1.1(24) \times 10^{-8}$
1	35–65–35	$5.1779(26) \times 10^{-2}$	1.1×10^{-8}
1	37–63–37	$4.8973(14) \times 10^{-2}$	$8.0(17) \times 10^{-9}$
2	35–63–35	$5.1361(27) \times 10^{-2}$	$1.3(5) \times 10^{-8}$
2	35–65–35	$5.1260(24) \times 10^{-2}$	1.3×10^{-8}
2	37–63–37	$4.8503(9) \times 10^{-2}$	1.0×10^{-8}

[a] No data were available for isotopomers 37–65–37, in levels 1 and 2.

This fact is illustrated by the efficiency of the correction factor ϵ, discussed above.

Force constants k_1 and k_{12} of $^{63}Cu^{35}Cl_2$ are deduced from values of ω_1 and ω_3 provided by the polynomial fit, using the VFF formulae applied to a linear XY_2 molecule [13]. We find $k_1==277.28(1)$ N m^{-1} and $k_{12}=7.37(1)$ N m^{-1}. The weakness of the interaction constant k_{12} justifies the use of the VFF approach. The limits of this model are obvious from the rms bias described above. Results [16] in the millimeter and submillimeter-wave range on $^{63}Cu^{35}Cl$, give $k_1=359.29(7)$ N m^{-1} from $\omega_e=417.60(4)$ cm^{-1}. Hence Cu-Cl bonding is significantly stronger in this species than in copper dichloride. This difference is calculated to be smaller in $NiCl_2$ for instance [17].

The bond length r_e is deduced from the ground state rotational constant given in table 3. Our value of B_e $(Cu^{35}Cl_2)=0.0582990(31)$ cm^{-1} gives $r_e=0.203335(5)$ nm, which compares quite well with the value quoted by Barnes et al. [12].

5. Conclusion

A complete set of molecular parameters has been obtained for the four symmetrical isotopomers of copper dichloride, assuming a VFF-linear XY_2 molecular force model for isotopic shifts, coupled to a simple polynomial expression for the v_1, v_3, and J rovibrational energy levels of the observed ground state. A small correction on the symmetric stretch isotopic factor gave a significant improvment in the quality of the fit. The rms deviation has been compared with a level-by-level procedure, revealing the occurrence of weak perturbations. Force constants k_1, k_{12} and the Cu-Cl bond length have been calculated and compared to values from other sources.

Further work remains to be done on $CuCl_2$: bending combination bands involving $v_2=2$ ground state levels have been detected recently in enriched $^{63}Cu^{37}Cl_2$ samples and are presently being analysed. We mentioned in fig. 3b of ref. [10] that when we populated level $v'=2$ with rhodamine 6G dye laser, rotational doublets involving vibrational combinations $1_{v_1-3n}3_{2n}$ $(n=1, 2, 3, 4)$ appear in the LIF-STF spectra with intensities comparable (sometimes higher) than the $1_{v_1}3_0$ main band. This might be explained by a coupling between the vibrational stretching modes, and work is in progress to check this hypothesis. Several problems remain unsolved in the spectroscopic investigation of this molecule, for example the origin of the red continuum detected in the LIF spectra shown in fig. 2 of ref. [10], the vibrational structure of the upper electronic state, and the observation of the other low-lying ligand field states: $^2\Pi_{g(1/2)}$, $^2\Sigma_g^+$.

Acknowledgment

We thank B. Erba, who prepared the isotopically enriched cells. We are also grateful to Dr. J.M. Brown and his group for fruitful discussions and communication of data from their $CuCl_2$ molecular beam experiments prior to publication. The Fourier transform interferometer was financed jointly by the CNRS, Université Lyon I, the Région Rhône Alpes, and DRET (grant 901609).

References

[1] J.T. Hougen, G.E. Leroi and T.C. James, J. Chem. Phys. 34 (1961) 1670.

[2] C.W. Bauschlicher and B.O. Roos, J. Chem. Phys. 91 (1989) 4785.

[3] S. Yoshida, M. Taniwaki, T. Sawano, K. Shimizu and T. Fujioka, J. Appl. Phys. Japan 28 (1989) L831.

[4] T. Tokuda, N. Fujii, S. Yoshida, K. Shimizu and I. Tanaka, Chem. Phys. Letters 174 (1990) 385.

[5] R. Bacis, J. Bonnet, A.J. Bouvier, P. Crozet, S. Churassy, E. Georges, B. Erba, J. Lamarre, Y. Louvet, M. Nota, D. Pigache, A.J. Ross and M. Setra, Europhys. Letters 12 (1990) 569.

[6] A.J. Bouvier, R. Bacis, J. Bonnet, S. Churassy, P. Crozet, B. Erba, J.B. Koffend, J. Lamarre, M. Lamrini, D. Pigache and A.J. Ross, Chem. Phys. Letters 184 (1991) 133.

[7] A.J. Bouvier, R. Bacis, J. Bonnet, S. Churassy, P. Crozet, B. Erba, J.B. Koffend, J. Lamarre, M. Lamrini, D. Pigache and A.J. Ross, J. Phys. (Paris) III 1 (1991) C7-663.

[8] H.P. Yang, Y. Qin, T.J. Cui, Q.N. Yuan, X.B. Xie, Q. Zhuang and C.H. Zhang, Chem. Phys. Letters 191 (1992) 130.

[9] T. Tokuda and N. Fujii, J. Phys. Chem. 96 (1992) 6504.

[10] A.J. Ross, R. Bacis, A.J. Bouvier, S. Churassy, J.C. Coste, P. Crozet and I. Russier, J. Mol. Spectry. 158 (1993) 27.

[11] F. Dienstbach, F.P. Emmenegger and C.W. Schläpfer, Helv. Chim. Acta 60 (1977) 2460.

[12] M.P. Barnes, R.T. Carter, N.M. Lakin and J.M. Brown, J. Chem. Soc. Faraday Trans. 89 (1993) 3205.

[13] G. Herzberg, Molecular spectra and molecular structure, Vol. 2 (Van Nostrand, New York, 1966).
[14] G. Herzberg, Molecular spectra and molecular structure, Vol. 3 (Van Nostrand, New York, 1966).
[15] J.K.G. Watson, J. Mol. Spectry. 80 (1980) 411.
[16] E.C. Manson, F.C. De Lucia and W. Gordy, J. Chem. Phys. 62 (1975) 1040.
[17] F.J. Grieman, S.H. Ashworth, J.M. Brown and I.R. Beattie, J. Chem. Phys. 92 (1990) 6365.
[18] J.M. Hollas, High resolution spectroscopy (Butterworths, London, 1982).